

1 Functional diversity reduces the risk of hydraulic 2 failure in tree mixtures through hydraulic disconnection

3

4 Myriam Moreno ^{1,2,*}, Guillaume Simioni ¹, Hervé Cochard ³, Claude Doussan ⁴, Joannès
5 Guillemot ^{5,6,7}, Renaud Decarsin ¹, Pilar Fernandez ¹, Jean-Luc Dupuy ¹, Santiago Trueba
6 ⁸, François Pimont¹, Julien Ruffault ¹, and Nicolas K. Martin-StPaul ¹

7

8

9 ¹URFM, INRAE, 84914 Avignon, France

10 ²French Environment and Energy Management Agency, 49000 Angers, France

11 ³PIAF, INRAE, Université Clermont Auvergne, 63000 Clermont-Ferrand, France

12 ⁴EMMAH, INRAE, 84914 Avignon, France

13 ⁵UMR Eco&Sols, CIRAD, 34398 Montpellier, France

14 ⁶Eco&Sols, Univ Montpellier, CIRAD, INRAE, IRD, Montpellier SupAgro, 34398
15 Montpellier, France

16 ⁷Department of Forest Sciences, ESALQ, University of São Paulo, Piracicaba, São
17 Paulo, Brazil

18 ⁸BIOGECO, INRAE, Université de Bordeaux, 33615 Pessac, France

19

20

21

22 * Myriam Moreno (corresponding author).

23 **Email:** myriam.moreno@inrae.fr

24

25

26

27

28

29

30

31

32

33 Abstract

34 Forest ecosystems are increasingly threatened by anthropogenic pressures, especially by
35 the increase in drought frequency and intensity. Tree species mixtures could improve
36 resilience to diverse global anthropogenic pressures. However, there is still little
37 consensus on how tree diversity affects water stress. Although some studies suggest that
38 mixing species with different drought response strategies could be beneficial, the
39 underlying mechanisms have seldom been identified. By combining a greenhouse
40 experiment and a soil-plant-atmosphere hydraulic model, we explored whether mixing a
41 drought avoidant (*Pinus halepensis*) and a drought tolerant (*Quercus ilex*) tree species
42 could reduce plant water stress (defined as the risk of hydraulic failure) during extreme
43 drought, compared to their respective monocultures. Our experiment showed that mixing
44 species with divergent drought response strategies had a neutral effect on the drought-
45 avoidant species and a positive effect on the drought-tolerant species. The model
46 simulations further suggested that the beneficial effect of mixture on plant water stress
47 during extreme drought was related to changes in the hydraulic connection of the plant
48 from both the soil and the atmosphere. The ability of the drought-avoidant species to
49 disconnect from the soil and the atmosphere limits its exposure to water stress, whereas
50 the ability of the drought-tolerant species to increase its hydraulic connection to the soil
51 lowers its hydraulic risk. This study brings a new insight on the mechanisms and traits
52 combinations improving drought resistance in diversified forests and plantations, with
53 important implications for forest management under climate change.

54
55

56 **Keywords**

57 Forest, functional diversity, drought resistance, tree hydraulic, safety margins.

58
59

60 **Main Text**

61 **Introduction**

62

63 The rising frequency and intensity of extreme drought is impacting tree survival and
64 forest functions worldwide (Allen et al., 2010; Breshears et al., 2013; Senf et al., 2020),
65 jeopardizing crucial forest ecosystem services. Tree species diversity has been promoted
66 as an important nature-based solution to improve the resilience of forests and tree
67 plantations (Messier et al., 2022). The effects of species mixing on drought resistance
68 could result from different mechanisms, such as competitive reduction for water through
69 resource partitioning or facilitation – for instance hydraulic redistribution (Grossiord,
70 2020). Yet, there is no consensus regarding the effects of tree diversity on forest
71 resistance to drought (Grossiord et al., 2014; Grossiord, 2020). Indeed, recent review
72 showed that diversity can have positive (de-Dios-García et al., 2015; Lebougeois et al.,
73 2013; Ruiz-Benito et al., 2017), neutral (Grossiord et al., 2014; Merlin et al., 2015) or
74 even negative impacts (C. Grossiord et al., 2014; Vitali et al., 2018). These conflicting
75 results suggest that it is not the species richness that matters, but rather the functional

76 composition (i.e., species with different drought response strategies) of the mixtures
77 (Forrester and Bauhus, 2016; Grossiord, 2020). Such hypothesis was supported by recent
78 research that found that the diversity of hydraulic traits determines the resilience to
79 drought of forest water fluxes globally (Anderegg et al., 2018; Haberstroh and Werner,
80 2022). Similarly, results from a large-scale tree diversity experiment showed that the
81 diversity of drought resistance strategies is a good predictor of the stability of tree growth
82 and forest productivity (Schnabel et al., 2021). However, we crucially miss a mechanistic
83 understanding of the way the diversity of drought resistance strategies mediates tree
84 mortality under extreme drought.

85 Tree drought resistance strategies result from a set of functional traits that determine how
86 rapidly the different tree functions will be impaired by drought stress (often quantified as
87 water potential thresholds inducing dysfunction). In particular, it determines the risk of
88 xylem hydraulic failure, caused by a high rate of embolism in xylem conduits (Tyree and
89 Sperry, 1989), which is a leading mechanism in drought-induced tree mortality (Adams et
90 al., 2017). It is common in the literature to distinguish species strategies based on
91 stomatal regulation - and associated water potential dynamics - and the xylem
92 vulnerability to embolism (Chen et al., 2021). Drought-tolerant species tend to maintain
93 gas exchanges during drought by delaying stomatal regulation, which implies important
94 soil water depletion and large decrease in the soil and tree water potential during drought
95 (Delzon, 2015; López et al., 2021). Their high resistance to xylem embolism limits the
96 risk of hydraulic failure. By contrast, drought-avoidants are generally more vulnerable to
97 xylem embolism, but they close their stomata earlier during drought, thereby reducing
98 soil water depletion, which in turn limits the soil and tree water potential decrease and the
99 risk of hydraulic failure (Delzon, 2015; López et al., 2021).

100 By assuming that trees are hydraulically connected to the soil (*i.e.*, soil and tree water
101 potential are at equilibrium if transpiration is null such as under predawn conditions) and
102 that the root system fully occupies a given soil volume, one can hypothesize how mixing
103 species with distinct drought response strategies impacts soil and tree water potentials,
104 and the risk of hydraulic failure under extreme drought:

105 **H1.** For a drought-tolerant species, it should be beneficial to compete for water with a
106 drought-avoidant neighbour, because the soil water saved by earlier stomatal regulation
107 of the avoidant is available to delay the decrease in water potential and the overall
108 hydraulic failure risk (Fig. 1).

109 **H2.** When grown in mixture with a drought tolerant neighbour, a drought-avoidant
110 species should be disadvantaged, as it would experience lower soil water potential due to
111 sustained water-use by the companion tolerant species. This would lead to a decrease in
112 its water potential, thereby increasing the risk of hydraulic failure (Fig. 1). The scenario
113 presented in Fig. 1 - which suggests that a drought tolerant always “win the fight” during
114 drought under mixture - holds only if the water potential of the mixed species is at
115 equilibrium with the soil water potential.

116 **H3.** If the root systems of the two neighbour species are segregated in space, water
117 consumption by the tolerant species does not affect the avoidant species and difference of
118 water potentials between tree species in the mixture could occur given their isolation

119 (Fig. 1). In support to this hypothesis, root niche separation is often assumed in the
120 literature to explain coexistence between co-occurring species (Grossiord, 2020; Jose et
121 al., 2006).

122 To test these hypotheses, we conducted a greenhouse experiment where seedlings of
123 *Pinus halepensis*, a drought avoidant (Baquedano and Castillo, 2007) and *Quercus ilex*, a
124 drought tolerant (Baquedano and Castillo, 2007) were grown in pairs in small pots (12 L).
125 Seedlings were planted in either monoculture or mixture with or without root separation.
126 We applied an extreme drought by stopping the watering and we regularly monitored the
127 overall pot soil (Ψ_{soil}) and tree predawn (Ψ_{pd}) water potentials, along with soil resistivity
128 and tree gas exchanges. These data were combined with a state-of-the-art soil-tree-
129 atmosphere hydraulic model (Cochard et al., 2021) to further identify the mechanisms
130 and traits involved in the co-existence of drought avoidant/tolerant species during
131 extreme drought.

132

133 Results and Discussion

134

135 **a) Empirical evidence for hydraulic commensality between *Quercus ilex* and**
136 ***Pinus halepensis* during extreme drought**

137 Tree predawn water potential (Ψ_{pd}) decreased markedly during drought (SI appendix,
138 Table S1, P-value < 0.001), but the dynamics differed between species across treatments
139 (SI appendix, Table S1, P-value < 0.001). Due to their differential drought resistance
140 strategies, Ψ_{pd} reached more negative values in the drought tolerant *Q. ilex* than in the
141 drought avoidant *P. halepensis*, regardless of the pot composition. In agreement with
142 hypothesis H1, *Q. ilex* had significantly more negative Ψ_{pd} in monoculture than in
143 mixture at the drought peak (Fig. 2A; SI appendix, Table S2, P-value < 0.01), except for
144 the mixture with root separation. By contrast, in *P. halepensis*, Ψ_{pd} at the drought peak
145 remained above both soil water potential (Ψ_{soil}) and *Q. ilex*'s Ψ_{pd} in mixture (Fig. 2A),
146 contradicting hypothesis H2.

147 Therefore, the hydraulic risk, estimated as the hydraulic safety margins at the drought
148 peak (HSM, computed as the difference between P50, the water potential causing 50%
149 xylem embolism and the average Ψ_{pd} at the driest date) was significantly improved in
150 mixture compared to monoculture only for *Q. ilex* (Fig. 2B). Hence, as expected from
151 hypothesis H1, the mixture had a positive effect on the reduction of the risk of hydraulic
152 failure for the drought tolerant species *Q. ilex* but contrary to hypothesis H2, the mixture
153 had a neutral effect on the drought avoidant *P. halepensis*. This result reflects a
154 commensalism relationship in terms of hydraulic risk between drought avoidant and
155 tolerant species under drought conditions, that to our knowledge, has never been
156 demonstrated until now. Hence, coexistence between a drought avoidant and a drought
157 tolerant species is not the exclusive result of spatial segregation of their root niche, even
158 if such phenomenon can occur (Bello et al., 2019), but depend rather on other
159 mechanisms that we further discuss below.

160 **b) Species coexistence relies on species-specific modifications of the soil-tree**
161 **hydraulic conductance**

162 The relationship between Ψ_{pd} and Ψ_{soil} (Fig. 3) in *P. halepensis* was unaffected by
163 mixture, with Ψ_{pd} equal to Ψ_{soil} until Ψ_{soil} decreased below -4 MPa. For Ψ_{soil} lower than -
164 4 MPa, Ψ_{pd} remained constant at ca. -4 MPa. For *Q. ilex* the slope between Ψ_{pd} and Ψ_{soil}
165 was greater than one (> 1.7 , Fig. 3) for monocultures and for the mixture with root
166 separation. By contrast, the slope of the Ψ_{pd} - Ψ_{soil} relationship was equal to one for *Q. ilex*
167 in mixture without root separation (i.e., $\Psi_{pd} \sim \Psi_{soil}$ throughout the experiment, Fig. 3).
168 Overall, these empirical results indicate that (i) the Ψ_{pd} vs. Ψ_{soil} relationships varied
169 between the two studied species with different drought resistance strategies and (ii) plant-
170 soil water potentials were modified by mixture only in *Q. ilex*, the drought tolerant
171 species.

172 It could be assumed that differences between Ψ_{pd} and Ψ_{soil} reflect shifts in the root profile
173 in mixtures compared to monocultures. Indeed, if roots explore only a part of the
174 available soil, Ψ_{pd} would equilibrate with this soil subspace, possibly differing from the
175 overall Ψ_{soil} measured at plot level. However, we used small pots (12 L) to impose a
176 complete occupation of the whole soil volume by the trees' root system, making this
177 assumption unlikely. Furthermore, the fact that we found no significant differences
178 between the average soil resistivity at the top and bottom profiles of the pots for each
179 modality suggests that water is absorbed uniformly throughout the soil and definitely
180 rules out this hypothesis (SI appendix, Fig. S1). Alternatively, we can postulate that
181 differences between Ψ_{pd} and Ψ_{soil} result from changes in the hydraulic conductance
182 between the soil and the trees.

183 Following the experimental component of our study, we carried out simulations with the
184 hydraulic process-based model SurEau (Cochard et al., 2021) to test the possible
185 mechanisms that could explain such empirical patterns. The model computes the water
186 fluxes along the soil-tree-atmosphere continuum by accounting for the different
187 resistances of the soil, the symplasm and apoplasm of the root, trunk, branch and leaf,
188 and calculate the water potential and the water content of the corresponding
189 compartments. By considering xylem vulnerability to cavitation, the model can estimate
190 the loss of hydraulic conductance of the tree xylem in relation to water potentials and
191 predicts the death of the tree by hydraulic failure when 100 % loss of hydraulic
192 conductivity is reached. The model was improved to represent two different individuals
193 competing for a same amount of soil water (see Materials and Methods).

194 We first conducted three benchmark simulations corresponding to Figure 1
195 (monocultures of *Q. ilex* and *P. halepensis* and the mixture without root separation). In
196 such simulations, we assumed that the hydraulic conductance of the rhizosphere (K_{rhizo})
197 and of the fine roots (K_{root}) were the same for all species and pot compositions. More
198 specifically, we applied the widespread "single root" approach that assumes that soil
199 conductivity relates to the soil water content (van Genuchten, 1980) and is scaled up to
200 the rhizosphere according to the length of fine roots per unit soil volume (Gardner, 1964;
201 I. R. Cowan, 1965)

202 By doing so, the model predicted behaviours consistent with our initial hypotheses H1
203 and H2 (Fig. 1): the drop of Ψ_{pd} in *P. halepensis* and *Q. ilex* growing in mixture are
204 respectively faster and slower than for the corresponding monocultures (Fig. 4A),
205 indicating that mixture should have a negative effect on *P. halepensis* and a positive

206 effect on *Q. ilex*, which contradict our results. We thus conducted sensitivity analyses on
207 different traits to explore mechanisms explaining our empirical observations.

208 **c) The drought-avoider *P. halepensis* isolates from the soil through a decrease
209 in both root hydraulic and cuticular conductance**

210 The fact that *P. halepensis* exhibits higher Ψ_{pd} than Ψ_{soil} during drought suggests that (i)
211 this species can isolate from the soil (i.e., reducing the soil to tree hydraulic conductance)
212 and (ii) is able to limit its dehydration. Several studies have suggested that plant isolation
213 from the soil allows limiting the exposure to water stress (Aguadé et al., 2015; Brito et
214 al., 2019; Cuneo et al., 2016). Different non-exclusive belowground mechanisms were
215 proposed to explain tree isolation from the soil, such as the formation of cortical lacunae
216 under fine roots (Cuneo et al., 2021; Duddek et al., 2022), which reduces water transfer to
217 the root stele and hence affect roots hydraulic conductance. Roots shrinkage might also
218 explain the plant-soil hydraulic disconnection by creating gaps between soil and fine
219 roots interrupting the hydraulic conductance between both interfaces. Furthermore, the
220 inhibition of the synthesis of proteins such as aquaporins facilitating water transport in
221 the transcellular pathway (Domec et al., 2021), or even fine roots mortality (Leonova et
222 al., 2022), could also explain hydraulic isolation. To evaluate whether tree isolation from
223 the soil could explain the observed water potential patterns in *P. halepensis*, we
224 hypothesized in the model a decrease in root hydraulic conductance (K_{root}) as the tree
225 water potential decreases (SI appendix, Fig. S2). Simulations were performed under a
226 mixture condition with *Q. ilex* as a companion species (parametrized as in benchmark
227 simulations) (Fig. 4B). This allows to force soil water potential to drop even after *P.*
228 *halepensis* has closed its stomata and has isolated from the soil. Model simulations
229 indicate that reducing only K_{root} does not allow to simulate higher Ψ_{pd} than Ψ_{soil} for *P.*
230 *halepensis* (Fig. 4B). This means that the water losses that occur after stomatal closure –
231 which result from the leaf cuticular conductance (g_{cuti}), set in the model using the average
232 value measured for *P. halepensis*, was high enough to cause tree water potential drops
233 after a strong decrease in K_{root} (Fig. 4B). We thus implemented in the model a down-
234 regulation of g_{cuti} with decreasing tree relative water content, which is in accordance with
235 empirical data obtained in *P. halepensis* using the drought-box methods (Billon et al.,
236 2020) (SI appendix, Fig. S3). Simulations showed that, although the reduction of g_{cuti}
237 alone attenuated the decrease in tree water potentials, the tree keeps dehydrating. Finally,
238 when implementing a decrease of both K_{root} and g_{cuti} under drought, *P. halepensis* water
239 potential departs from soil water potentials (Fig. 4B), in line with our observations. This
240 suggests that these two mechanisms jointly could allow *P. halepensis* to prevent
241 dehydration under drought. In the natural forest context, tree isolation from the soil
242 during drought has already been proposed to explain the coexistence of drought-avoidant
243 and drought-tolerant trees (Aguadé et al., 2015; Moreno et al., 2021; Pangle et al., 2012;
244 Plaut et al., 2012). Yet, to our knowledge, the mechanisms leading to complete plant
245 disconnection from the soil and the atmosphere had never been proposed until now.

246 **d) The drought-tolerant *Quercus ilex* increases root hydraulic conductance to
247 the soil in mixture through increased root length**

248 For *Q. ilex*, Ψ_{pd} was respectively lower or comparable to Ψ_{soil} under monoculture and
249 mixture conditions (Fig. 2A) which suggests that (i) contrary to *P. halepensis*, *Q. ilex* is

250 not able to limit its dehydration and (ii) the mixture likely impact the hydraulic
251 conductance between the soil and the trees under drought.

252 According to the diffusion law, the lower departure between Ψ_{pd} and Ψ_{soil} that we
253 observed for *Q. ilex* in mixture compared to monoculture, could result from an increase in
254 the conductance of the rhizosphere, which could lower the water potential drops required
255 for a given flux between the soil and the tree (39).

256 As we found a greater root system length in mixture than in monoculture (SI appendix,
257 Fig. S4), we assumed that the increase in rhizosphere conductance might be achieved
258 through an increase in exchange surface between soil and root (“single root” approach).
259 We tested this hypothesis by varying the modelling parameters of fine roots length per
260 unit soil volume. This sensitivity test shows that changing K_{rhizo} can change the Ψ_{pd} vs
261 Ψ_{soil} relationships between monoculture and mixture (Fig. 4C). Indeed, reducing the value
262 of this parameter (graph “root length x ½”, Fig. 4C), results in a departure between Ψ_{pd}
263 and Ψ_{soil} as observed in monoculture, whereas increasing it results in Ψ_{pd} and Ψ_{soil} being
264 comparable, as observed in mixture. Interestingly, some studies have already reported
265 modifications of the root system under mixture toward higher fine roots density (Sun et
266 al., 2017; Wambsganss et al., 2021), identifying this phenomenon to a complementarity
267 effect between species associated.

268 **e) Ecological implications**

269 Our results provide evidence that mixing drought-avoidant and drought-tolerant species
270 reduces the risk of hydraulic failure under extreme drought conditions at the community
271 level. According to model simulations, such mixing effect can be explained by changes in
272 hydraulic connection between the plant, the soil and the atmosphere during drought. The
273 avoidant species can sustain extreme drought through an isolation from the soil (decrease
274 of K_{root}) and the atmosphere (decrease of g_{cuti}) whereas the tolerant species can increase
275 hydraulic conductance of the rhizosphere through an increase in root length. Such results
276 remained to be tested at larger scale but could change our view about the mechanisms of
277 species co-existence. Whereas it is sometimes assumed that mixture has positive effect
278 due to root system segregation in space (Bello et al., 2019; Grossiord et al., 2018), we
279 provide evidence that the hydraulic connection of the plant to the soil and the atmosphere
280 can also be involved, without the need to call for a spatial segregation of the root systems.

281 Our results also challenge the way vegetation models represent drought stress. To date,
282 the majority of process-based models assume that soil water deficit in the rooting zone
283 drives the water status of the plant. However, we provide evidence that changes in
284 hydraulic connection from the soil can make the plant behave independently from soil
285 water status. Implementing such processes in larger scale vegetation models could help
286 explain and predict co-existence between species and drought induced effect on forest
287 community. Such modelling approach could be a step toward the development of tools
288 allowing to design drought resilient mixture.

289

290

291

292 Materials and Methods

293 Seedlings and experimental design

294 The experiment was set up during the summer 2021. It consisted in applying a drought
295 treatment (watering stop) to potted *P. halepensis* and *Q. ilex* trees grown in monoculture
296 or in mixture while monitoring ecophysiological variables at 5 different dates. Seedlings
297 of *P. halepensis* and *Q. ilex* (one- and two-years old respectively) of equivalent
298 dimensions were repotted in January 2020. 90 trees of each species were planted in 12 L
299 containers, including two individuals per pot, either in monoculture or in mixtures. The
300 soil was composed of sand (~20%) and organic matters. Half of the pots were equipped
301 with a physical barrier made of acrylic fabric (with 30µm mesh) that precludes root
302 colonization from one side to the other of the pot but allow water transfer between the
303 two separated compartments. From 2019 to June 2021, saplings were grown at the
304 National Forestry Office of France (ONF) nursery in Cadarache (Southeast of France)
305 and were watered twice a week to field capacity and fertilized once a week. One month
306 before the start of the experiment (June 2021), pots were brought on the campus of
307 INRAe (Avignon, France) to acclimate in the experimental greenhouse. The greenhouse
308 was equipped with air temperature, a humidity (HD 9817T1) and radiation loggers. It
309 included an independent regulation of climate through aeration (opening of the glasses or
310 forced ventilation in the compartment) and cooling (humidification of the air entering
311 through a “cool□ box”). These systems allowed regulating the environment of the
312 greenhouse according to the defined settings. In addition, the sidewalls of the greenhouse
313 have been whitewashed to homogenize the radiation and the temperature. The
314 temperature was kept between 25 and 35 °C, relative humidity (RH) between 40 and
315 75%, and maximum diurnal photosynthetically active radiation (PAR) below 1000
316 µmol.m⁻². s⁻¹ (SI appendix, Fig. S5).

317 During acclimation period, watering was applied as in the nursery. Among the initial
318 batch of 90 pots, we selected 54 pots for which the two trees were alive and had reached
319 a height between 40 and 60 cm with less than 10cm heights differences between the two
320 trees. Pots were divided into two batches: a batch of 6 pots per composition (36 pots in
321 total) that was assigned to the drought experiment, and a batch of 3 pots per treatment (18
322 pots in total) that was assigned to a control treatment in which trees were maintained
323 watered all along the season (two times a week). All pots were monitored once a week,
324 from July 26 to August 18, for soil water and water potential and ecophysiological
325 variables (leaf water potentials, leaf gas exchange, pots water loss- described below). The
326 day before the beginning of the experiment, at the end of the afternoon, all pots were
327 watered at saturation and weighted.

328

329 Tree water potentials

330 Water potential was estimated through leaf water potentials of all trees measured at
331 predawn once a week across the experimental period..The evening before measurements,
332 for each tree, one leaf (*Q. ilex*) or small twig (*P. halepensis*) was covered with an
333 aluminium foil and placed in a ziplock plastic bag. In addition, to limit tree nocturnal
334 transpiration and allow water potential equilibration between the tree and the soil

335 (Rodriguez-Dominguez et al., 2022), trees were covered with a plastic bag and a piece of
336 wet paper was included under the plastic bag. Samples were collected before sunrise,
337 between 4 to 5 am, kept into the ziplock and immediately placed in a cooler for water
338 potential measurement. The 108 measurements were done randomly in less than 4 hours
339 following sampling, with a scholander pressure chamber (PMS model 1505 D). At the
340 beginning of the experimentation, midday water potentials of tree were measured
341 between 1 and 2 PM, following the same procedures as described above for predawn
342 water potential (leaf or twig covered with an aluminium foil and placed in a ziplock
343 plastic bag). There were used to parametrize the model.

344

345 **Tree leaf gas exchanges**

346 Leaf level gas exchange was measured using two portable photosynthesis system (LI-
347 6400XT) for all trees at all dates except the second one due to breakdown of the
348 greenhouse system. Measurements were done between 11 am to 3 pm, period during
349 which PAR in the green house is highest and stable (between 600 and 1000 $\mu\text{mol.m}^{-2}. \text{s}^{-1}$).
350 Licor chamber conditions were set to keep close to the greenhouse while providing
351 non-limiting conditions: PAR was set at 1000 $\mu\text{mol.m}^{-2}. \text{s}^{-1}$, the block temperature was
352 set at 25°C, flow rate and scrubbing were adjusted to maintain RH between 60 and 80%.
353 The leaves were allowed to acclimate for at least 3 minutes in the chamber before
354 measurement, to ensure gas exchange stability. For each leaf (*Q. ilex*) or needle bunch (*P. halepensis*),
355 ten values were recorded during one minute and the average was used in the
356 data analysis. After the measurement, the area of leaves or needles included in the
357 chamber were cut and stored in a plastic bag inside a cooler. The day after, leaf area was
358 measured to correct gas exchange computation with actual leaf area in the chamber.
359 Samples were then dried during 48 hours at 70°C to estimate specific leaf area.

360

361 **Tree biomass and leaf area estimates**

362 We estimated leaf area of each tree at the beginning and the end of the experiment using
363 a method relying on profile photographs, proposed by (Michael and Parker, 2000). It is
364 based on a calibrated relationship between the projected area of the tree profile and the
365 foliage biomass estimated destructively. For each species, we first built a calibration
366 relationship between numbers of tree pixels in profile photographs and the foliage
367 biomass. For the calibration relationship, trees were selected to span the range of sizes
368 encountered in the experiment. We sampled trees before the beginning of the drought
369 experiment (June 2021), and after the experiment (September 2021) to consider potential
370 changes in size or leaf area or angulation that could have occurred during the summer and
371 influenced the relationship. For each tree, the profile surface projected area was estimated
372 by photography. All the settings were made to ensure a constant reproduction ratio (i.e.,
373 constant dimensions of real object dimensions per pixel) among photographs. To obtain
374 foliage dry mass, all trees used for this calibration were cut at the base of the stem after
375 taking photographs. Tree parts were sorted to separate green foliage, dead foliage, and the
376 rest which is almost entirely made of stems. Tree parts were then dried at 70°C for 3 days
377 (leaves/ needles) or until there was no variation in dry mass (almost one week). The leaf

378 area of each tree with the estimation of total foliage dry mass at a specific date and
379 specific leaf area estimated on leaf gas exchange measurement samples.

380 At the end of the experiment and for droughted pots, the belowground part of each tree
381 were uprooted. The rooting system was washed to separate the soil particles for the roots.
382 The rooting system extension (maximal length and width) were measured using a ruler,
383 with a millimeter resolution. The root system was then dried out at 70°C in an oven for at
384 least 10 days, until there are no more weight variations, and the total dry mass was
385 estimated.

386

387 **Soil water content and soil water potentials**

388 Pots were weighted at each measurement dates in the morning (8am) and at the end of the
389 measurement day (5pm). Soil water content was estimated at the pot level, by subtracting
390 the total pot weight, performed at each measurement dates in the morning (ca. 8 am), the
391 soil dry mass and the total fresh tree biomass. Soil water potential (Ψ_{soil}) was then
392 estimated at the pot level from the normalized soil water content of the pots (W_{norm}) and
393 water retention curves determined in the laboratory on soil samples ($V = 6 \text{ cm}^3$). The
394 determination of the retention curve was made with the combination of suction table
395 ($\Psi_{soil} > -0.01 \text{ MPa}$), pressure plate ($\Psi_{soil} > -1.5 \text{ MPa}$) and dew point hygrometer (WP4C,
396 Decagon- $\Psi_{soil} < -1.5 \text{ MPa}$) methods (Dane and Hopmans, 2002). Five soil sample
397 replicates were used for each point of the retention curve and the gravimetric water
398 content was determined from fresh and dry weight obtained after drying in an oven at
399 70°C (limit temperature to avoid organic matter degradation) for about one week. To
400 perfectly match the data, two different retention curves were fitted. A first retention curve
401 was fitted with two set of van-Genuchten relationships (van Genuchten, 1980)
402 intersecting at a gravimetric water content of 0.116 g.g^{-1} (corresponding to $\Psi_{soil} = -1.4$
403 MPa). A second set of retention curve was fitted with only one van-Genuchten
404 relationships (van Genuchten, 1980). The retention curves take the following form:

$$\psi_{soil} = \frac{\left(\left(\frac{1}{W_{norm}} \right)^{\frac{1}{m}} - 1 \right)^{\frac{1}{n}}}{\alpha}$$

405 where m , n and α are empirical parameters describing the typical sigmoidal shape of the
406 function and W_{norm} is the normalized water content. Water potential was calculated from
407 this fit using the gravimetric water content of pots estimated at each measurement dates.
408 The parameters of the curves are provided in the SI appendix, Table S3.

409 The normalized water content was computed for each pot as:

$$W_{norm} = \frac{W - Wr}{Wsat - Wr}$$

410 With W the soil mass of the pot at a given time, Wr the soil mass at residual water
411 content. It was measured at the end of the experiment after drying the soil at 70°C. $Wsat$
412 is the saturated mass of the soil which was estimated from the first weight measurement

413 of the experiment, after the pots were irrigated at saturation. W and W_{sat} were computed
414 by removing the mass of the tree and the pot to the total weight measured during the
415 experiment (either from the balance or continuous load cell measurements). The total tree
416 fresh was measured at the end of the experiment, by assuming that tree growth that could
417 have occur during the experiment can be neglected due to the extreme drought
418 experienced by the tree. W_{norm} was not measured on the control (irrigated) pots.

419

420 **Soil resistivity measurement**

421 Electrical resistivity of soil in pots was measured using electrical resistivity tomography
422 (ERT). 4 pots (including one control) per modality (monoculture or mixture, with or
423 without root separation system) were selected. On these pots, electrical resistivity was
424 monitored with time over 2 radial planes, located at 1/3 and 2/3 of the pots' height, by
425 inserting 20 stainless steel screws (2cm long) equally spaced (3.9cm) along the column's
426 circumference. ERT measurement were done using an ABEM SAS 4000 resistivity meter
427 connected to all these electrodes. All quadrupole combinations were used, including
428 reciprocal measurements for assessing error and measurement quality. The resistivity
429 measurements were taken before the start of the experiment (when the pot substrates
430 were at field capacity), in the middle and at the end of the experiment. In the late dry
431 situations, it was necessary to add a small amount of water at electrodes to enable soil-
432 electrode electrical contact and resistivity measurements. Soil resistivity distribution at
433 the two heights was obtained from the inversion of apparent resistivity using ResIPy
434 software (Blanchy et al., 2020).

435

436 **Statistics**

437 We evaluated globally the effect of species and measurement date and their interaction on
438 the water potential of trees by using a linear mixed model. Then, for each species
439 independently and root separation modalities (root separation or not), we assessed the
440 effect of the pot composition (mixture or monoculture association) on tree water
441 potentials by considering date, composition and their interaction as explanatory factors.
442 As we did not find any significant differences between water potentials of monoculture
443 with and without root separation for each species (SI appendix, Fig. S6), we decided to
444 pool them for the analysis. We also test the differences between soil and water potentials
445 of tree at each measurement dates using Student T test. Finally, we applied post-hoc
446 Tukey HSD tests to evaluate differences between pots modalities (composition and root
447 separation modalities) for leaf area and gas exchanges variables (leaf conductance and
448 transpiration, Fig. S7). All statistical analyses were performed with the R software (3.5.2,
449 R Development Core Team 2018) with the package LME4 and *agricolae*.

450

451 **Model analysis using SurEau**

452 We used the SurEau model to explore how the species composition in pots influenced
453 soil and water potential dynamics during extreme drought (Cochard et al., 2021). SurEau
454 is a soil-tree-atmosphere model that simulates water fluxes and stocks with the soil-tree
455 atmosphere continuum by accounting for conductance, water potential gradient and

456 capacitances. It is dedicated to model extreme drought and accounts for the processes
457 occurring after the point of stomatal closure (*i.e.*, cuticular water losses and hydraulic
458 conductance and water stocks losses due to xylem embolism). It is discretized in the soil
459 layers and four tree compartments (roots, trunk, branches, and leaves) which are each
460 described by an apoplastic and a symplasmic water volume. At each time step, the
461 model computes leaf stomatal and cuticular transpiration as the product between leaf-to-
462 air vapor pressure deficit and stomatal and cuticular conductance. Knowing the soil water
463 content, soil water potential and hydraulic conductance are computed. This along with
464 leaf stomatal and cuticular fluxes, can be used to compute tree water potential in the
465 different tree compartments while accounting for the symplasmic capacitance and the
466 hydraulic conductance losses due to xylem embolism. The resulting water potential is
467 used to compute stomatal closure, water content, and xylem embolism. The model is
468 driven by hourly climate data, tree traits (water pools dimensions, stomatal response to
469 water potential, cuticular transpiration, capacitance, and vulnerability curve to cavitation
470 (SI appendix, Table S4) and soil properties (volume and water retention curves). In the
471 present study, the model was improved to include the possibility for two trees to absorb
472 water in the same soil volume. In principle, two codes corresponding to two trees,
473 parameterized for monoculture of *P. halepensis*, monoculture of *Q. ilex* or for mixture,
474 were run in parallel.

475 To test the hypotheses presented in the introduction (illustrated in Fig. 1) and evaluate
476 whether the model can also explain the patterns of soil and water potential dynamics
477 found experimentally. First, we performed *benchmark* simulations, for monoculture and
478 mixture, with default parameters, to reproduce the hypotheses presented in Figure 1. As
479 explained above, the patterns of Figure 1 hold only under the assumptions that (i) the two
480 individuals in the pots exploit the same soil water stock (physical coexistence of the
481 roots) and are perfectly connected to the soil (large hydraulic conductance between the
482 soil and the fine roots). In SurEau the flow of water between the soil and the roots is
483 modelled using two different types of conductance in series, (i) the hydraulic
484 conductance between the soil and the root surface (K_{soil}) which depends on fine roots
485 density and the soil water content (Martin-StPaul et al., 2017), and (ii) the hydraulic
486 conductance between the root surface and the inner root (K_{root}) which depends on the fine
487 roots area (R_a) and fine roots conductivity (K_{root}), both set constant by default (Cochard
488 et al., 2021). The first hypothesis (root occupy the same volume) was fulfilled by setting
489 the same quantity of fine roots in all three soil layers for the two individuals in the pot.
490 The second hypothesis (equilibration between tree and soil water potential) was fulfilled
491 by setting a fine roots length so that the soil hydraulic conductance is high enough for the
492 night-time water potential equalled the soil water potential all along the drought range
493 and before hydraulic failure (where water potential drops to minus infinity).

494 However, two different empirical results conflicted the expected patterns and we used the
495 model to explain the divergences observed.

496 Firstly, *P. halepensis* showed that water potential can be higher than soil water potential
497 during extreme drought under all composition monoculture and mixture, suggesting that
498 this species can behave independently from the soil and maintain its water potential
499 constant even if soil water potential decreases. Recent work suggests that disconductance
500 between the soil and root can occur for some species (Cuneo et al., 2016; Duddek et al.,

501 2022; North and Nobel, 1997). This can be represented in the model by decreasing the
502 root conductance relative to water potential in the root. We thus implemented an equation
503 relating the root hydraulic conductance to the root water potential (SI appendix, Fig. S2)
504 for *P. halepensis* and realized simulation in mixture conditions with *Q. ilex* parametrized
505 as in benchmark conditions. It appeared that this implementation led to an acceleration of
506 hydraulic failure for *P. halepensis*. This is explained by the excessive water losses, that
507 occur through the cuticle at this stage of water stress, and that cannot anymore be
508 compensated by the supply from the root. Under the same mixture conditions, we
509 therefore also tested whether a decrease in leaf cuticular conductance with relative water
510 content (RWC, SI Appendix, Fig. S3), a phenomenon already observed on cut branches
511 of *P. halepensis*, could explain -- alone or in combination with the reduction in root
512 conductance -- the observed pattern.

513 Secondly, for *Q. ilex*, we noticed lower water stress under mixture linked to a change of
514 the soil water potential (Ψ_{soil}) vs plant predawn water potential (Ψ_{pd}) relationship. Higher
515 plant water potential for a given soil water potential was found under mixture compared
516 to monoculture. Such pattern could be explained by an increase of the soil hydraulic
517 conductance that, as explained above, can be related to the density of fine roots (L_a , the
518 length of fine roots per m² of soil). We thereby performed a sensitivity analysis on this
519 trait under monoculture conditions to support that its variation could explain the
520 empirical observation.

521

522 **References**

523 Adams, H.D., Zeppel, M.J.B., Anderegg, W.R.L., Hartmann, H., Landhäusser, S.M.,
524 Tissue, D.T., Huxman, T.E., Hudson, P.J., Franz, T.E., Allen, C.D., Anderegg,
525 L.D.L., Barron-Gafford, G.A., Beerling, D.J., Breshears, D.D., Brodribb, T.J.,
526 Bugmann, H., Cobb, R.C., Collins, A.D., Dickman, L.T., Duan, H., Ewers, B.E.,
527 Galiano, L., Galvez, D.A., Garcia-Forner, N., Gaylord, M.L., Germino, M.J.,
528 Gessler, A., Hacke, U.G., Hakamada, R., Hector, A., Jenkins, M.W., Kane, J.M.,
529 Kolb, T.E., Law, D.J., Lewis, J.D., Limousin, J.M., Love, D.M., Macalady, A.K.,
530 Martínez-Vilalta, J., Mencuccini, M., Mitchell, P.J., Muss, J.D., O'Brien, M.J.,
531 O'Grady, A.P., Pangle, R.E., Pinkard, E.A., Piper, F.I., Plaut, J.A., Pockman, W.T.,
532 Quirk, J., Reinhardt, K., Ripullone, F., Ryan, M.G., Sala, A., Sevanto, S., Sperry,
533 J.S., Vargas, R., Vennetier, M., Way, D.A., Xu, C., Yepez, E.A., McDowell, N.G.,
534 2017. A multi-species synthesis of physiological mechanisms in drought-induced
535 tree mortality. *Nat Ecol Evol* 1, 1285–1291. <https://doi.org/10.1038/s41559-017-0248-x>

537 Aguadé, D., Poyatos, R., Rosas, T., Martínez-Vilalta, J., Aguadé, D., Poyatos, R., Rosas,
538 T., Martínez-Vilalta, J., 2015. Comparative Drought Responses of *Quercus ilex* L.
539 and *Pinus sylvestris* L. in a Montane Forest Undergoing a Vegetation Shift. *Forests*
540 6, 2505–2529. <https://doi.org/10.3390/f6082505>

541 Allen, C.D., Macalady, A.K., Chenchouni, H., Bachelet, D., McDowell, N., Vennetier,
542 M., Kitzberger, T., Rigling, A., Breshears, D.D., Hogg, E.H. (Ted), Gonzalez, P.,

543 Fensham, R., Zhang, Z., Castro, J., Demidova, N., Lim, J.H., Allard, G., Running,
544 S.W., Semerci, A., Cobb, N., 2010. A global overview of drought and heat-induced
545 tree mortality reveals emerging climate change risks for forests. *For Ecol Manage*
546 259, 660–684. <https://doi.org/10.1016/j.foreco.2009.09.001>

547 Anderegg, W.R.L., Konings, A.G., Trugman, A.T., Yu, K., Bowling, D.R., Gabbitas, R.,
548 Karp, D.S., Pacala, S., Sperry, J.S., Sulman, B.N., Zenes, N., 2018. Hydraulic
549 diversity of forests regulates ecosystem resilience during drought. *Nature* 561, 538–
550 541. <https://doi.org/10.1038/s41586-018-0539-7>

551 Baquedano, F.J., Castillo, F.J., 2007. Drought tolerance in the Mediterranean species
552 *Quercus coccifera*, *Quercus ilex*, *Pinus halepensis*, and *Juniperus phoenicea*.
553 *Photosynthetica* 45. <https://doi.org/10.1007/s11099-007-0037-x>

554 Bello, J., Hasselquist, N.J., Vallet, P., Kahmen, A., Perot, T., Korboulewsky, N., 2019.
555 Complementary water uptake depth of *Quercus petraea* and *Pinus sylvestris* in
556 mixed stands during an extreme drought. *Plant Soil* 437.
557 <https://doi.org/10.1007/s11104-019-03951-z>

558 Billon, L.M., Blackman, C.J., Cochard, H., Badel, E., Hitmi, A., Cartailler, J., Souchal,
559 R., Torres-Ruiz, J.M., 2020. The DroughtBox: A new tool for phenotyping residual
560 branch conductance and its temperature dependence during drought. *Plant Cell
561 Environ* 43, 1584–1594. <https://doi.org/10.1111/PCE.13750>

562 Blanchy, G., Saneiyan, S., Boyd, J., McLachlan, P., Binley, A., 2020. ResIPy, an intuitive
563 open source software for complex geoelectrical inversion/modeling. *Comput Geosci*
564 137. <https://doi.org/10.1016/j.cageo.2020.104423>

565 Breshears, D.D., Adams, H.D., Eamus, D., McDowell, N.G., Law, D.J., Will, R.E.,
566 Williams, A.P., Zou, C.B., 2013. The critical amplifying role of increasing
567 atmospheric moisture demand on tree mortality and associated regional die-off.
568 *Front Plant Sci*. <https://doi.org/10.3389/fpls.2013.00266>

569 Brito, C., Dinis, L.-T., Moutinho-Pereira, J., Correia, C.M., 2019. Drought Stress Effects
570 and Olive Tree Acclimation under a Changing Climate. *Plants (Basel)* 8.
571 <https://doi.org/10.3390/plants8070232>

572 Chen, Z., Zhang, Y., Yuan, W., Zhu, S., Pan, R., Wan, X., Liu, S., 2021. Coordinated
573 variation in stem and leaf functional traits of temperate broadleaf tree species in the
574 isohydric-anisohydric spectrum. *Tree Physiol* 41.
575 <https://doi.org/10.1093/treephys/tpab028>

576 Cochard, H., Pumont, F., Ruffault, J., Martin-StPaul, N., 2021. SurEau: a mechanistic
577 model of plant water relations under extreme drought. *Ann For Sci* 78, 1–23.
578 <https://doi.org/10.1007/S13595-021-01067-Y/TABLES/7>

579 Cuneo, I.F., Barrios-Masias, F., Knipfer, T., Uretsky, J., Reyes, C., Lenain, P., Brodersen,
580 C.R., Walker, M.A., McElrone, A.J., 2021. Differences in grapevine rootstock

581 sensitivity and recovery from drought are linked to fine root cortical lacunae and
582 root tip function. *New Phytologist* 229. <https://doi.org/10.1111/nph.16542>

583 Cuneo, I.F., Knipfer, T., Brodersen, C.R., McElrone, A.J., 2016. Mechanical failure of
584 fine root cortical cells initiates plant hydraulic decline during drought. *Plant Physiol*
585 172. <https://doi.org/10.1104/pp.16.00923>

586 Dane, J.H., Hopmans, J.W., 2002. Methods of Soil Analysis, Part 4, Physical Methods,
587 in: Soil Science Society of America Book Series. Madison.

588 de-Dios-García, J., Pardos, M., Calama, R., 2015. Interannual variability in competitive
589 effects in mixed and monospecific forests of Mediterranean stone pine. *For Ecol
590 Manage* 358, 230–239. <https://doi.org/10.1016/J.FORECO.2015.09.014>

591 Delzon, S., 2015. New insight into leaf drought tolerance. *Funct Ecol* 29, 1247–1249.
592 <https://doi.org/10.1111/1365-2435.12500>

593 Domec, J.C., King, J.S., Carmichael, M.J., Overby, A.T., Wortemann, R., Smith, W.K.,
594 Miao, G., Noormets, A., Johnson, D.M., 2021. Aquaporins, and not changes in root
595 structure, provide new insights into physiological responses to drought, flooding,
596 and salinity. *J Exp Bot* 72. <https://doi.org/10.1093/jxb/erab100>

597 Duddek, P., Carminati, A., Koebernick, N., Ohmann, L., Lovric, G., Delzon, S.,
598 Rodriguez-Dominguez, C.M., King, A., Ahmed, M.A., 2022. The impact of
599 drought-induced root and root hair shrinkage on root–soil contact. *Plant Physiol.*
600 <https://doi.org/10.1093/plphys/kiac144>

601 Forrester, D.I., Bauhus, J., 2016. A Review of Processes Behind Diversity—Productivity
602 Relationships in Forests. *Current Forestry Reports* 2, 45–61.
603 <https://doi.org/10.1007/S40725-016-0031-2/FIGURES/3>

604 Gardner, W.R., 1964. Relation of Root Distribution to Water Uptake and Availability 1 .
605 *Agron J* 56. <https://doi.org/10.2134/agronj1964.00021962005600010013x>

606 Grossiord, C., 2020. Having the right neighbors: how tree species diversity modulates
607 drought impacts on forests. *New Phytologist* 228, 42–49.
608 <https://doi.org/10.1111/NPH.15667>

609 Grossiord, C., Gessler, A., Granier, A., Pollastrini, M., Bussotti, F., Bonal, D., 2014.
610 Interspecific competition influences the response of oak transpiration to increasing
611 drought stress in a mixed Mediterranean forest. *For Ecol Manage* 318, 54–61.
612 <https://doi.org/10.1016/j.foreco.2014.01.004>

613 Grossiord, C., Sevanto, S., Bonal, D., Borrego, I., Dawson, T.E., Ryan, M., Wang, W.,
614 McDowell, N.G., 2018. Prolonged warming and drought modify belowground
615 interactions for water among coexisting plants. *Tree Physiol* 39.
616 <https://doi.org/10.1093/treephys/tpy080>

617 Grossiord, Granier, A., Ratcliffe, S., Bouriaud, O., Bruelheide, H., Chećko, E., Forrester,
618 D.I., Dawud, S.M., Finér, L., Pollastrini, M., Scherer-Lorenzen, M., Valladares, F.,

619 Bonal, D., Gessler, A., 2014. Tree diversity does not always improve resistance of
620 forest ecosystems to drought. *Proceedings of the National Academy of Sciences*
621 111, 14812–14815. <https://doi.org/10.1073/pnas.1411970111>

622 Haberstroh, S., Werner, C., 2022. The role of species interactions for forest resilience to
623 drought. *Plant Biol.* <https://doi.org/10.1111/PLB.13415>

624 I. R. Cowan, 1965. Transport of Water in the Soil-Plant-Atmosphere System. *Journal of*
625 *Applied Ecology* 2, 221–239.

626 Jose, S., Williams, R., Zamora, D., 2006. Belowground ecological interactions in mixed-
627 species forest plantations. *For Ecol Manage* 233.
628 <https://doi.org/10.1016/j.foreco.2006.05.014>

629 Lebougeois, F., Gomez, N., Pinto, P., Mérian, P., 2013. Mixed stands reduce *Abies alba*
630 tree-ring sensitivity to summer drought in the Vosges mountains, western Europe.
631 *For Ecol Manage* 303, 61–71. <https://doi.org/10.1016/J.FORECO.2013.04.003>

632 Leonova, A., Heger, A., Vásconez Navas, L.K., Jensen, K., Reisdorff, C., 2022. Fine root
633 mortality under severe drought reflects different root distribution of *Quercus robur*
634 and *Ulmus laevis* trees in hardwood floodplain forests. *Trees - Structure and*
635 *Function* 36. <https://doi.org/10.1007/s00468-022-02275-3>

636 López, R., Cano, F.J., Martin-StPaul, N.K., Cochard, H., Choat, B., 2021. Coordination
637 of stem and leaf traits define different strategies to regulate water loss and tolerance
638 ranges to aridity. *New Phytologist* 230. <https://doi.org/10.1111/nph.17185>

639 Martin-StPaul, N., Delzon, S., Cochard, H., 2017. Plant resistance to drought depends on
640 timely stomatal closure. *Ecol Lett* 20, 1437–1447.

641 Merlin, M., Perot, T., Perret, S., Korboulewsky, N., Vallet, P., 2015. Effects of stand
642 composition and tree size on resistance and resilience to drought in sessile oak and
643 Scots pine. *For Ecol Manage* 339, 22–33.
644 <https://doi.org/10.1016/J.FORECO.2014.11.032>

645 Messier, C., Bauhus, J., Sousa-Silva, R., Auge, H., Baeten, L., Barsoum, N., Bruelheide,
646 H., Caldwell, B., Cavender-Bares, J., Dhiedt, E., Eisenhauer, N., Ganade, G.,
647 Gravel, D., Guillemot, J., Hall, J.S., Hector, A., Hérault, B., Jactel, H., Koricheva, J.,
648 Kreft, H., Mereu, S., Muys, B., Nock, C.A., Paquette, A., Parker, J.D., Perring,
649 M.P., Ponette, Q., Potvin, C., Reich, P.B., Scherer-Lorenzen, M., Schnabel, F.,
650 Verheyen, K., Weih, M., Wollni, M., Zemp, D.C., 2022. For the sake of resilience
651 and multifunctionality, let's diversify planted forests! *Conserv Lett* 15.
652 <https://doi.org/10.1111/conl.12829>

653 Michael, T.-M., Parker, W., 2000. Estimating biomass of white spruce seedlings with
654 vertical photo imagery. *New For (Dordr)* 145–162.
655 <https://doi.org/10.1023/A:1006716406751>

656 Moreno, M., Simioni, G., Cailleret, M., Ruffault, J., Badel, E., Carrière, S., Davi, H.,
657 Gavinet, J., Huc, R., Limousin, J.-M.M., Marloie, O., Martin, L., Rodríguez-
658 Calcerrada, J., Vennetier, M., Martin-StPaul, N., 2021. Consistently lower sap
659 velocity and growth over nine years of rainfall exclusion in a Mediterranean mixed
660 pine-oak forest. *Agric For Meteorol* 308–309, 108472.

661 North, G.B., Nobel, P.S., 1997. Drought-induced changes in soil contact and hydraulic
662 conductivity for roots of *Opuntia ficus-indica* with and without rhizosheaths. *Plant*
663 *Soil* 191. <https://doi.org/10.1023/A:1004213728734>

664 Pangle, R.E., Hill, J.P., Plaut, J.A., Yepez, E.A., Elliot, J.R., Gehres, N., McDowell,
665 N.G., Pockman, W.T., 2012. Methodology and performance of a rainfall
666 manipulation experiment in a piñon-juniper woodland. *Ecosphere* 3, art28.
667 <https://doi.org/10.1890/ES11-00369.1>

668 Plaut, J.A., YEPEZ, E.A., Hill, J., Pangle, R., SPERRY, J.S., Pockman, W.T., McDowell,
669 N.G., Ssperry, J.S., Pockman, W.T., McDowell, N.G., 2012. Hydraulic limits
670 preceding mortality in a piñon-juniper woodland under experimental drought. *Plant*
671 *Cell Environ* 35, 1601–1617. <https://doi.org/10.1111/j.1365-3040.2012.02512.x>

672 Rodriguez-Dominguez, C.M., Forner, A., Martorell, S., Choat, B., Lopez, R., Peters,
673 J.M.R., Pfautsch, S., Mayr, S., Carins-Murphy, M.R., McAdam, S.A.M.,
674 Richardson, F., Diaz-Espejo, A., Hernandez-Santana, V., Menezes-Silva, P.E.,
675 Torres-Ruiz, J.M., Batz, T.A., Sack, L., 2022. Leaf water potential measurements
676 using the pressure chamber: Synthetic testing of assumptions towards best practices
677 for precision and accuracy. *Plant Cell Environ* 45, 2037–2061.
678 <https://doi.org/10.1111/PCE.14330>

679 Ruiz-Benito, P., Ratcliffe, S., Jump, A.S., Gómez-Aparicio, L., Madrigal-González, J.,
680 Wirth, C., Kändler, G., Lehtonen, A., Dahlgren, J., Kattge, J., Zavala, M.A., 2017.
681 Functional diversity underlies demographic responses to environmental variation in
682 European forests. *Global Ecology and Biogeography* 26, 128–141.
683 <https://doi.org/10.1111/GEB.12515>

684 Schnabel, F., Liu, X., Kunz, M., Barry, K.E., Bongers, F.J., Bruelheide, H., Fichtner, A.,
685 Härdtle, W., Li, S., Pfaff, C.-T., Schmid, B., Schwarz, J.A., Tang, Z., Yang, B.,
686 Bauhus, J., von Oheimb, G., Ma, K., Wirth, C., 2021. Species richness stabilizes
687 productivity via asynchrony and drought-tolerance diversity in a large-scale tree
688 biodiversity experiment. *Sci Adv* 7, 11–13. <https://doi.org/10.1126/sciadv.abk1643>

689 Senf, C., Buras, A., Zang, C.S., Rammig, A., Seidl, R., 2020. Excess forest mortality is
690 consistently linked to drought across Europe. *Nat Commun* 11, 6200.
691 <https://doi.org/10.1038/s41467-020-19924-1>

692 Sun, Z., Liu, X., Schmid, B., Bruelheide, H., Bu, W., Ma, K., 2017. Positive effects of
693 tree species richness on fine-root production in a subtropical forest in SE-China.
694 *Journal of Plant Ecology* 10. <https://doi.org/10.1093/jpe/rtw094>

695 Tyree, M.T., Sperry, J.S., 1989. Vulnerability of Xylem to Cavitation and Embolism.
696 Annu Rev Plant Physiol Plant Mol Biol 40, 19–36.
697 <https://doi.org/10.1146/annurev.pp.40.060189.000315>

698 van Genuchten, M.Th., 1980. A Closed-form Equation for Predicting the Hydraulic
699 Conductivity of Unsaturated Soils. Soil Science Society of America Journal 44,
700 892–898. <https://doi.org/10.2136/SSAJ1980.03615995004400050002X>

701 Vitali, V., Forrester, D.I., Bauhus, J., 2018. Know Your Neighbours: Drought Response
702 of Norway Spruce, Silver Fir and Douglas Fir in Mixed Forests Depends on Species
703 Identity and Diversity of Tree Neighbourhoods. Ecosystems 2017 21:6 21, 1215–
704 1229. <https://doi.org/10.1007/S10021-017-0214-0>

705 Wambsganss, J., Beyer, F., Freschet, G.T., Scherer-Lorenzen, M., Bauhus, J., 2021.
706 Tree species mixing reduces biomass but increases length of absorptive fine
707 roots in European forests. Journal of Ecology 109.
708 <https://doi.org/10.1111/1365-2745.13675>

709 **Acknowledgments**

710

711 Myriam Moreno was supported by the French Environment and Energy Management
712 Agency (ADEME) in the form of a PhD scholarship. The experiment was funded by
713 Agence Nationale pour la Recherche (ANR Hydrauleaks, MixForChange) and the
714 Metaprogramme ACCAF Drought&Fire.

715

716 **Author Contributions**

717 M.M., N.M. and H.C designed the research; M.M., G.S., N.M. C.D, P.F and R.D.
718 performed research; H.C. and N.M. performed the model simulations; M.M analyzed the
719 data, with the help of N.M, G.S, and CD; M.M and N.M wrote the paper, and all authors
720 contributed to its review.

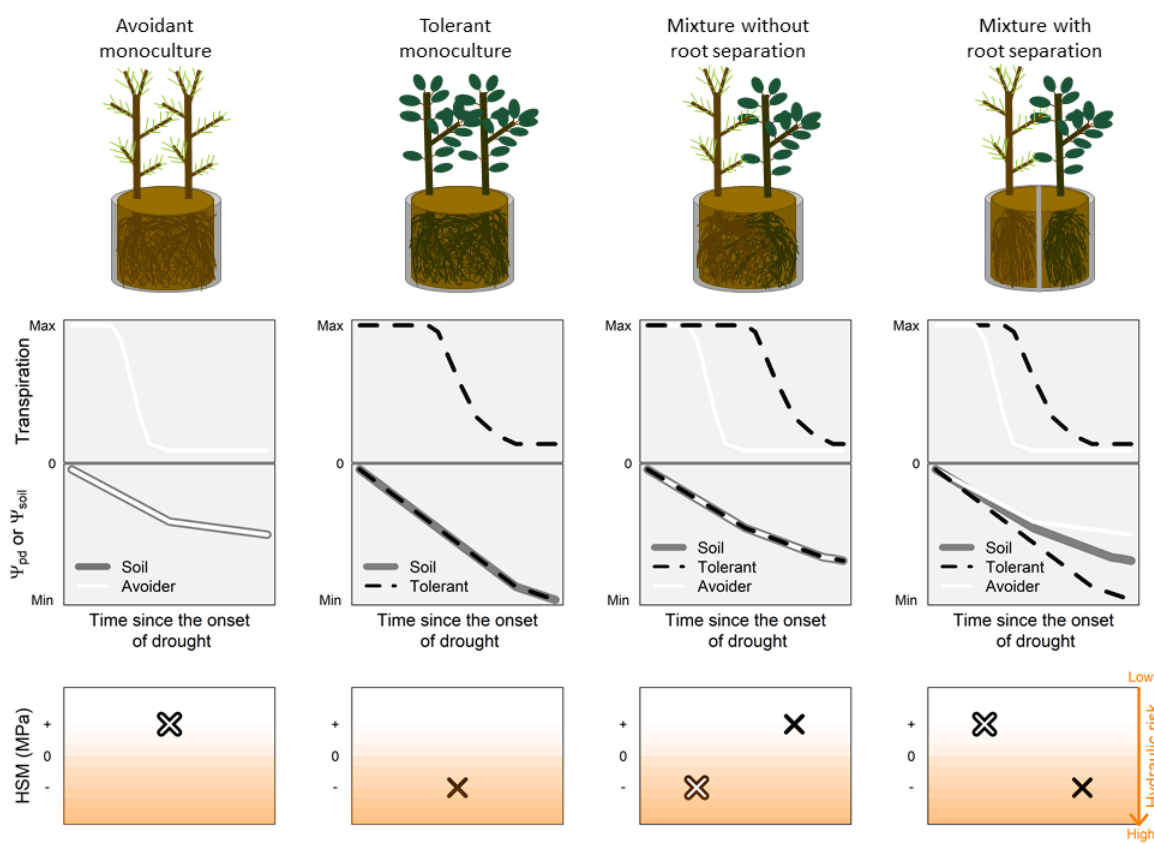
721

722 **Competing Interest Statement**

723 Authors declare no competing interest.

724 **Figures and Tables**

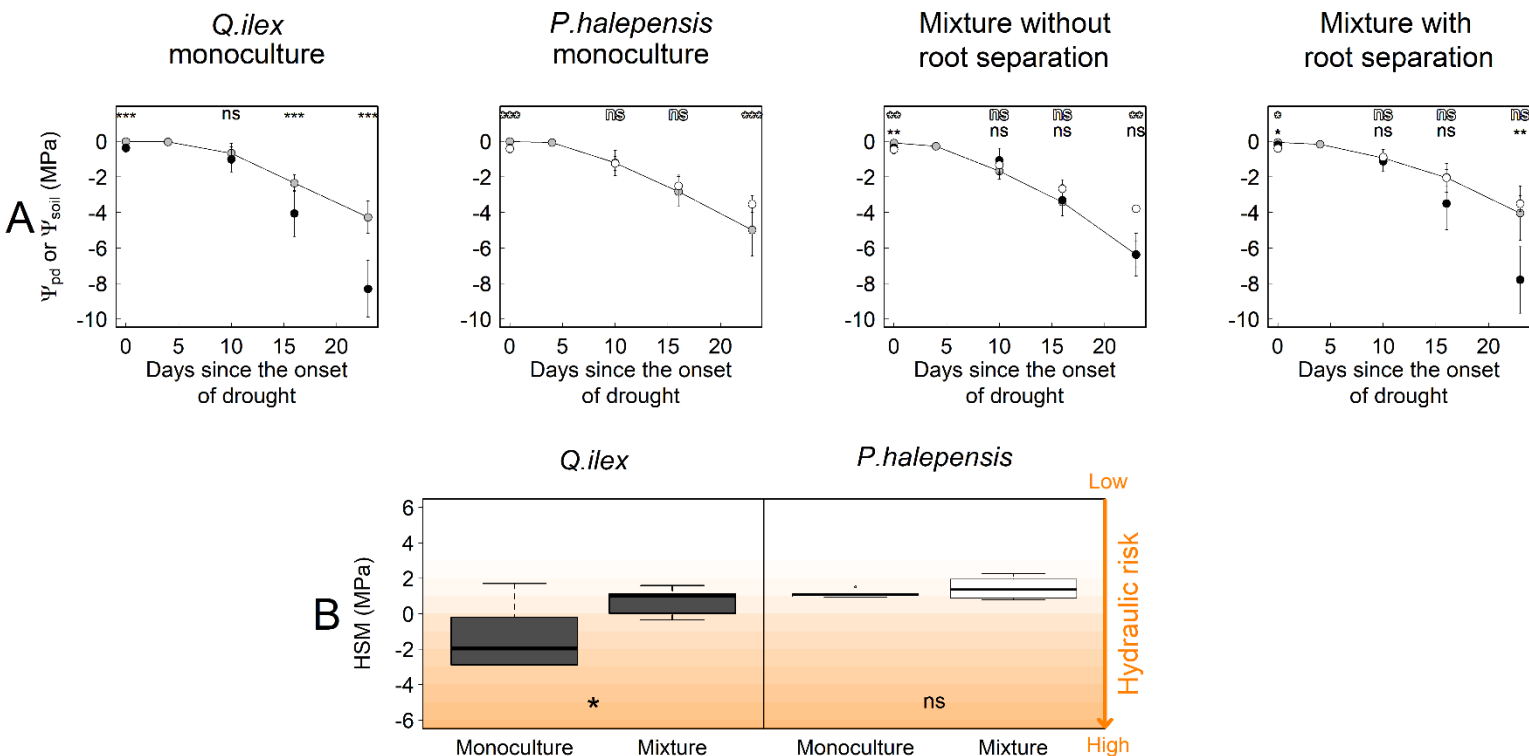
725



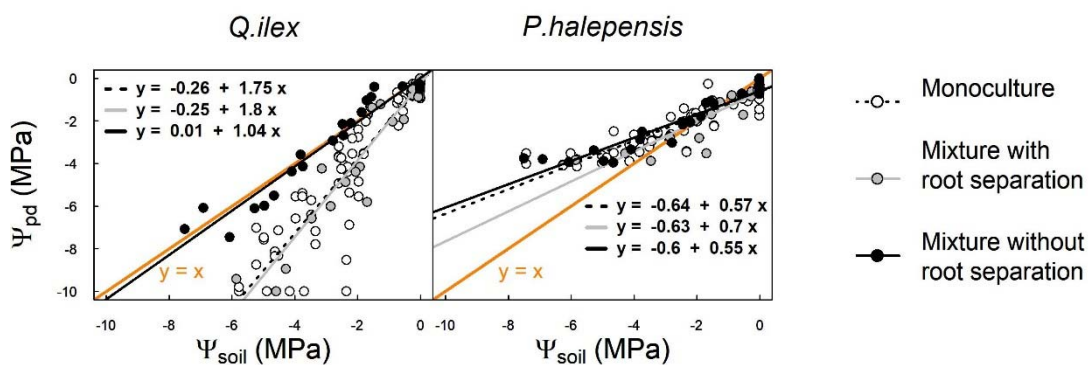
726

727

728 **Figure 1.** Experimental design and hypothesized drought responses for monoculture and
729 mixture of a drought avoider and a drought tolerant species. The transpiration, water
730 potentials (Ψ_{soil} : overall pot soil water potential; Ψ_{pd} : tree water potential) and hydraulic
731 safety margins (ie. HSM: the difference between Ψ_{pd} and P50; the water potential causing
732 50 % of embolism) expected according to pot modalities are presented. In the drought
733 avoidant monoculture, trees transpiration are expected to reduce rapidly after the onset of
734 drought, limiting Ψ_{soil} and Ψ_{pd} drop and hence hydraulic failure risk (positive HSM). In the drought
735 tolerant monoculture, transpiration of the two trees is expected to reduce later
736 than the one of the drought avoidant species, inducing a sharp decrease of Ψ_{soil} and Ψ_{pd} ,
737 increasing the risk of hydraulic failure (negative HSM). In the mixture without root
738 separation, transpiration of the drought avoidant species decreases earlier than for the
739 drought tolerant, which improve the water potential and HSM of the drought tolerant
740 compared to monoculture. However, because the two trees share the same volume of soil,
741 the water consumption of the drought tolerant should decrease water potential and HSM
742 of the drought avoidant thereby increasing its hydraulic failure risk compared to the
743 monoculture. A mixture with root separation illustrates that when each species root
744 system occupies its proper soil volume, the regulation of the transpiration, the water
745 potentials dynamics and the HSM are expected to be the same as in monoculture. As Ψ_{soil}
746 represents the global pot soil water potential, it is here equal to the mean of both
747 compartments soil water potential.



748 **Figure 2.** Positive and neutral effect of mixture on hydraulic failure risk of drought tolerant *Q. ilex* and drought avoidant *P.*
749 *halepensis*. (A) Soil and tree water potential for the different pot composition at each measurement dates. Soil water potentials
750 represent average values computed at the pot level from manual weightings (grey points). The average tree water potentials of *Q. ilex*
751 and *P. halepensis* correspond respectively to black and white dots. Standard deviations are represented and significant differences
752 between soil and water potentials are indicated (ns, non-significant differences; *, 0.01 \leq p $<$ 0.05; **, 0.001 \leq p $<$ 0.01; ***, p $<$
753 0.001). Per measurement date, for Ψ_{pd} , N = 24 for monoculture (pooling monoculture with and without root separation/ two trees per
754 pots) and 6 for mixture. For Ψ_{soil} , N = 12 for monoculture (pooling monoculture with and without root separation) and 6 for mixtures
755 concerning soil water potentials. (B) Hydraulic safety margins (HSM) measured at the driest date of the experiment in monoculture
756 (with and without root separation) and mixture (only for pots designed without root separation). HSM were computed as the difference
757 between water potential at the driest date and the P50 (i.e., the water potential causing 50% embolism).



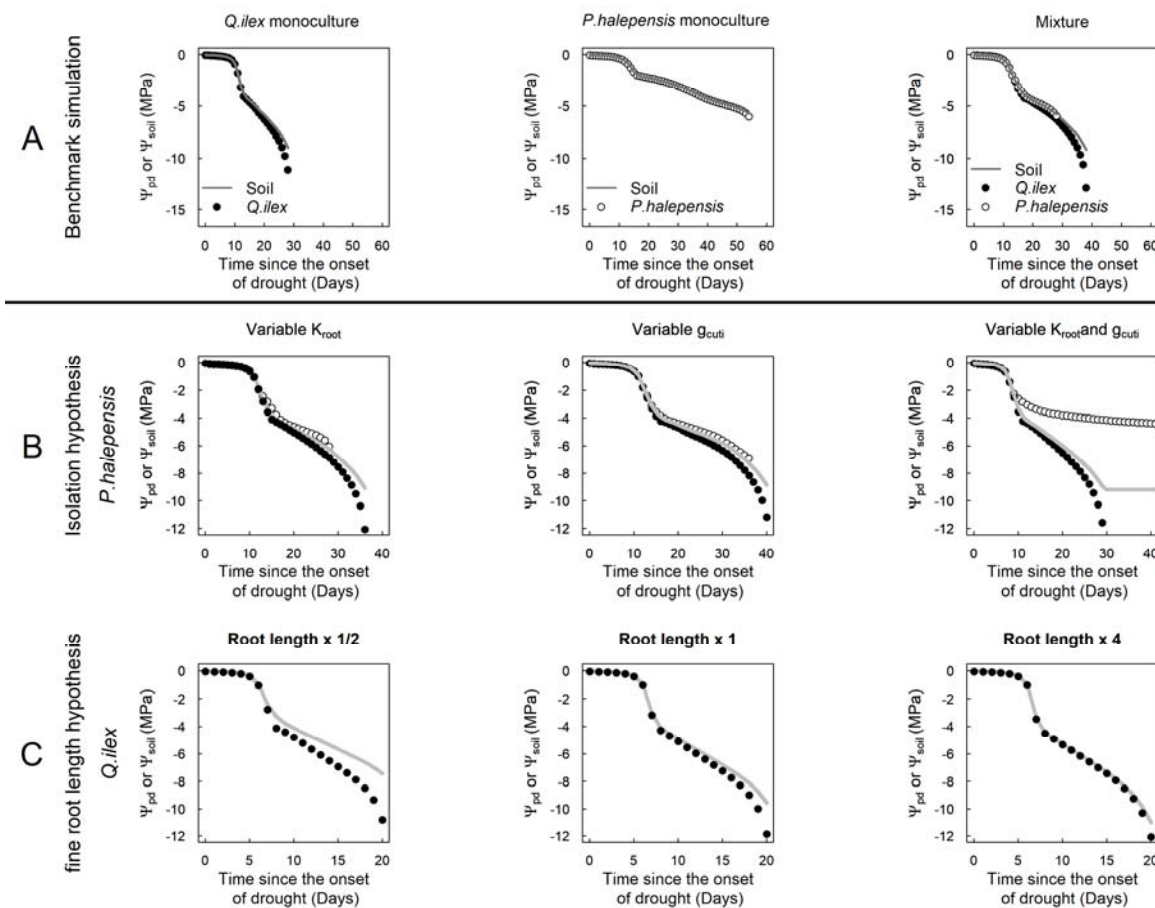
758

759

760

761 **Figure 3.** Uncoupling between soil and tree water potentials suggest an improvement of
762 the soil-tree hydraulic conductance for *Q. ilex* in mixture and soil isolation for *P. halepensis*. Different colours were used for monoculture (black dots), mixture with root
763 separation (light grey dots) and mixture without root separation (dark grey dots). The
764 isoline ($y=x$) is reported in orange line. For each modality, linear fit between soil and
765 water potentials is depicted and the equation is indicated on the plot. N = 96 for
766 monoculture (with and without root separation) and 24 for mixture for each root
767 separation categories.
768

769



770
771
772

773 **Figure 4.** Implication of the soil-tree hydraulic conductance in the coexistence of drought
774 avoidant and drought tolerant species during extreme drought. (A) Benchmark SurEau
775 simulations of the dynamics of leaf and soil water potentials for *P. halepensis* and *Q. ilex*
776 grown in monoculture and mixture until tree death. In these simulations root hydraulic
777 conductance and cuticular conductance were kept constant. The results are in adequation
778 with H1 and H2 hypotheses postulated in the introduction (illustrated in Fig.1). (B) Test
779 of sensibility of root conductance (K_{root}) and leaf cuticular conductance (g_{cuti}) parameters
780 for *P. halepensis*. By reducing both parameters, trees can keep higher water potentials
781 than the soil. (C) Test of sensibility of fine roots length parameter for *Q. ilex*
782 (multiplying fine roots length by $\frac{1}{2}$, 1 and 4). The more the fine roots length, the closer
783 are tree predawn and soil water potential. Note that the graduation of the x and y axis
784 change according to plot. Model parameters are provided in the SI appendix, Table S4.

785
786
787
788
789